We are IntechOpen, the world's leading publisher of Open Access books Built by scientists, for scientists

6,900
Open access books available

185,000
International authors and editors

200M
Downloads

Our authors are among the

154
Countries delivered to

TOP 1%
most cited scientists

12.2%
Contributors from top 500 universities



WEB OF SCIENCE™

Selection of our books indexed in the Book Citation Index in Web of Science™ Core Collection (BKCI)

Interested in publishing with us?
Contact book.department@intechopen.com

Numbers displayed above are based on latest data collected.
For more information visit www.intechopen.com



Chapter 3

Impurity Exclusion and Retention during Crystallisation and Recrystallisation — The Phenacetin by Ethylation of Paracetamol Process

Danielle E. Horgan, Lorraine M. Crowley,
Stephen P. Stokes, Simon E. Lawrence and
Humphrey A. Moynihan

Additional information is available at the end of the chapter

http://dx.doi.org/10.5772/59715

1. Introduction

A key issue facing the pharmaceutical and fine chemical industries is the generation of impurities during process chemistry and the retention, or otherwise, of these during crystallisation and subsequent processing. FDA guidelines [1] recognise organics, inorganics and residual solvents as possible impurities, and that organic impurities can arise during manufacturing or storage from starting materials, by-products, intermediates, degradation products, reagents, ligands and catalysts. Actual or potential impurities which can arise during synthesis, purification and storage must be noted and listed in the specification for any new drug substance. As crystallisation is the most important method of product isolation and purification in pharmaceutical manufacturing, the presence of impurities in the crystallisation medium or in the crystal product is clearly a significant issue. The presence of impurities in the crystalline product may affect the specification compliance of the batch. Any impurities present must be known, quantified and below specified limits. Impurities in the crystallisation medium can affect nucleation and growth rates, crystal form, including polymorphism or solvate formation, and morphology, including habit and crystal size distribution.

An example of the inter-relationship between process chemistry, impurities and crystallisation outcome is given by (*R,R*)-formoterol tartrate (1) [2]. The final step in the formation of this compound was salt formation which also resulted in the precipitation of a crystalline product. Compounds (2), (3), (4) and (5) in Figure 1 were identified as impurities in this material. Impurity (2) is a degradation product arising from hydrolysis of the formamide group of (1).

INTECH
open science | open minds

© 2015 The Author(s). Licensee InTech. This chapter is distributed under the terms of the Creative Commons Attribution License (http://creativecommons.org/licenses/by/3.0), which permits unrestricted use, distribution, and eproduction in any medium, provided the original work is properly cited.

Compounds (3), (4) and (5) arise as side-products of hydrogenation steps in the synthesis of (1). Three crystal forms of (*R,R*)-formoterol tartrate were identified, polymorphic forms A and B and a hydrate (form C). The initially precipitated material was form B and contained all four impurities in quantities of 0.04% to 0.64%, above the specified levels. Recrystallisation of the precipitated material gave crystals of form A, the thermodynamically preferred form, in which impurities (4) and (5) were no longer detectible, impurity (3) was reduced by 50%, but the levels of impurity (2) were increased due to further formamide degradation. Alternatively, warming the initially slurry of compound (1) resulted in significant redissolution of all four impurities, and formation of hydrate form C. Combination of re-slurrying and recrystallisation also gave low levels of all four impurities and solid material as the preferred crystal form A.

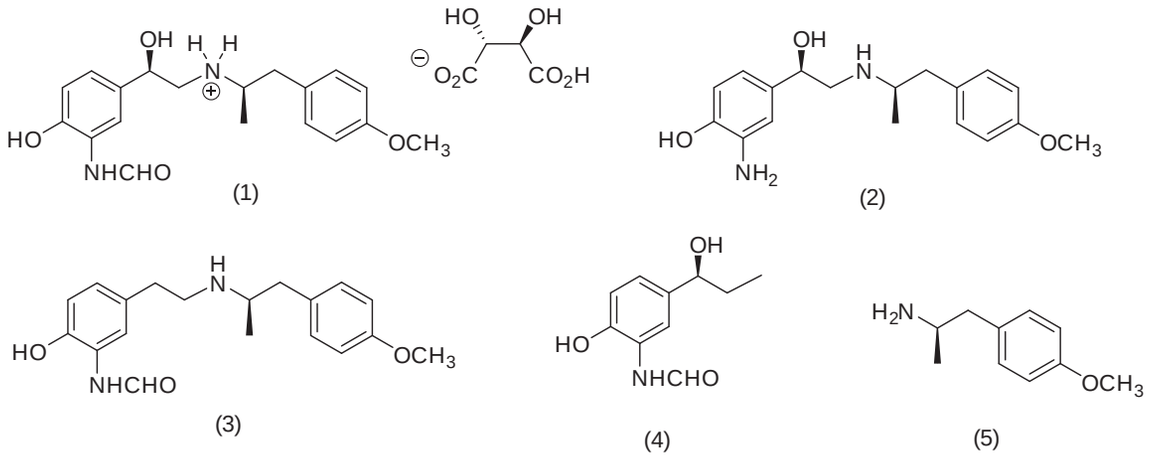


Figure 1. Molecular structure of (*R,R*)-formoterol tartrate (1) and impurity compounds (2), (3), (4) and (5) [2].

There are several examples in the literature of process impurities affecting polymorphic outcome. An excellent example concerns sulfathiazole (compound 7 in Figure 2), which is prepared by a process in which the final step is the hydrolysis of the acetamido precursor (6) [3]. Residual starting material (6) has a major impact on the polymorphic form of the resulting sulfathiazole solid, favouring form II. Crystallisation of pure sulfathiazole under identical conditions results in forms III or IV being obtained. This outcome was well rationalised on the basis of the hydrogen bonding networks present in the polymorphs and the capacity of the amide impurity (6) to interact with these. Another example concerns 5-haloaspirin derivatives (compounds 8 in Figure 3). These compounds are usually prepared by acetylation of the corresponding salicyclic acid derivatives. Anhydrides (9) are process intermediates and impurities in such reactions. Two polymorphs of compounds (8) have been noted, designated forms I and II. Impurity anhydrides (9) promote the formation of the form II polymorphs over forms I [4]. An example which has been studied in detail concerns an unidentified 'API X' (compound 10 in Figure 4) [5]. Three polymorphs of this compound are known, designated forms A, B and C. The crystal structures and supramolecular packing motifs of these forms have been fully characterised. A dimer involving H•••F hydrogen bonds (Figure 4) was one of the motifs found in forms A and B. A number of process impurities were found (Figure 5) and the impact of these on crystallisation of 'API X' investigated. For example, it was found

http://dx.doi.org/10.5772/59715

that impurities (11) and (12) (Figure 5) inhibited the transformation of form A to form B at 30 °C in IPA. Under these conditions, form B is the thermodynamically preferred form and batches of pure form A, or form A in the presence of impurities (13) or (14), transform to form B. It was noted that impurities (11) and (12) possess the molecular groups necessary for formation of a dimer motif of the type shown in Figure 4, whereas impurities (13) and (14) lack such groups. Impurities (11) and (12) can therefore mimic dimers of 'API X' and affect the polymorphic transformation.

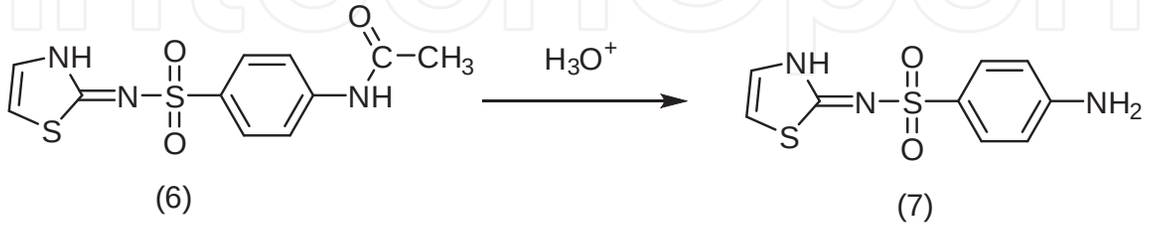


Figure 2. Final step in the preparation of sulfathiazole (7).

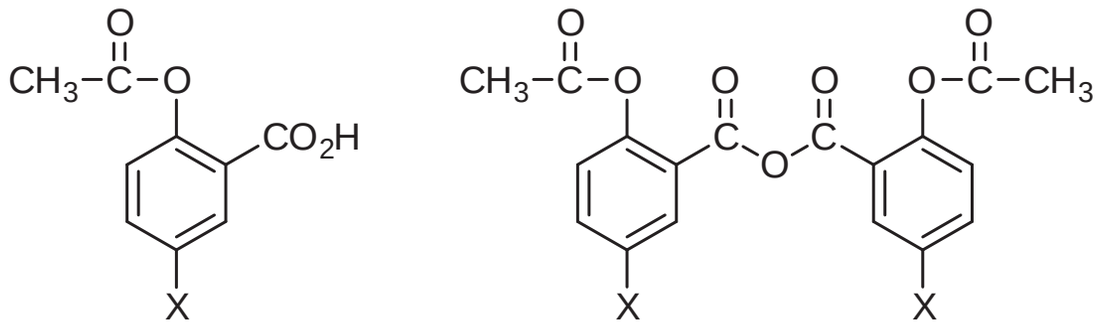


Figure 3. Structures of 5-haloaspirins (8) and corresponding anhydride impurities (9); X = Cl or Br.

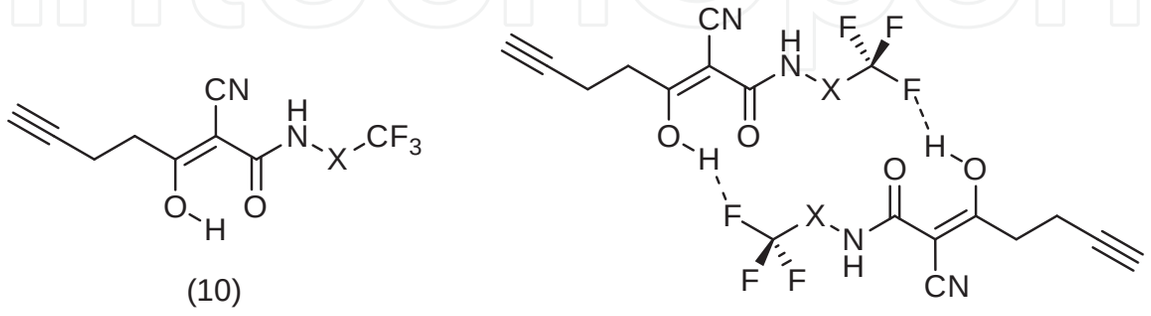
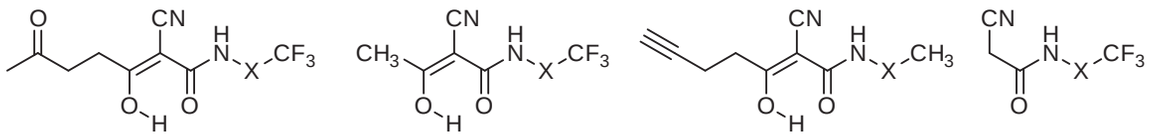


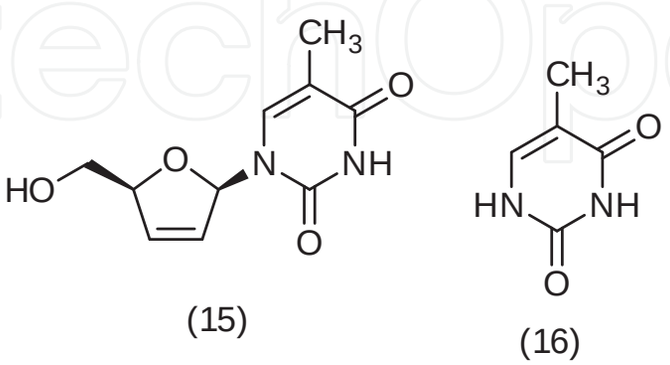
Figure 4. Structure of 'API X' (10). Group X, which is not a halogen, is unidentified in the publication [5]. On the right is a dimer motif of compound (10) present in polymorphs A and B involving H•••F hydrogen bonds.



(11) (12) (13) (14)

Figure 5. Process impurities present in the crystallisation of 'API X' [5].

Impurities can also have an effect on crystal morphology. For example, crystallisation of stavudine (compound 15 in Figure 6) from IPA gave needle-like crystals with sub-optimal filtration properties. Thymine (16), which can be present as a process impurity in quantities up to 1%, resulted in crystallisation of less acicular crystals with improved filtration properties [6]. The impact of impurities on crystal habits has been studied in detail in the case of benzamide (17). The most stable polymorph of benzamide crystallises from ethanol as plates which display the most growth in the *b* crystallographic direction; this direction also coincides with an 'amide ladder' motif (Figure 7). Impurities or additives which can engage with the amide ladder motif can affect the observed crystal habit. Benzoic acid (18) was found to reduce growth in the *b* crystallographic direction while 2-toluamide (19) was found to reduce growth in the *a* direction, giving smaller prisms elongated in the *a* and *b* directions respectively [7]. The presence of 2'-aminoacetophenone (20) was found to result in growth of polycrystalline benzamide aggregates as a consequence of compound (20) 'end-capping' the amide ladder motif, but also allowing for growth of a new benzamide crystallite [8]. Another example concerns phenyl salicylate (21). In this case, the concept of site-specific adsorption on crystal surfaces has been used to simulate adsorption with molecular modelling methods, to allow prediction of crystal morphology in the presence of impurities, giving good prediction of variation in habit due to phenyl benzoate (22), benzophenone (23) or benzhydrol (24) impurities [9].



(15) (16)

Figure 6. Molecular structures of stavudine (15) and thymine (16).

http://dx.doi.org/10.5772/59715

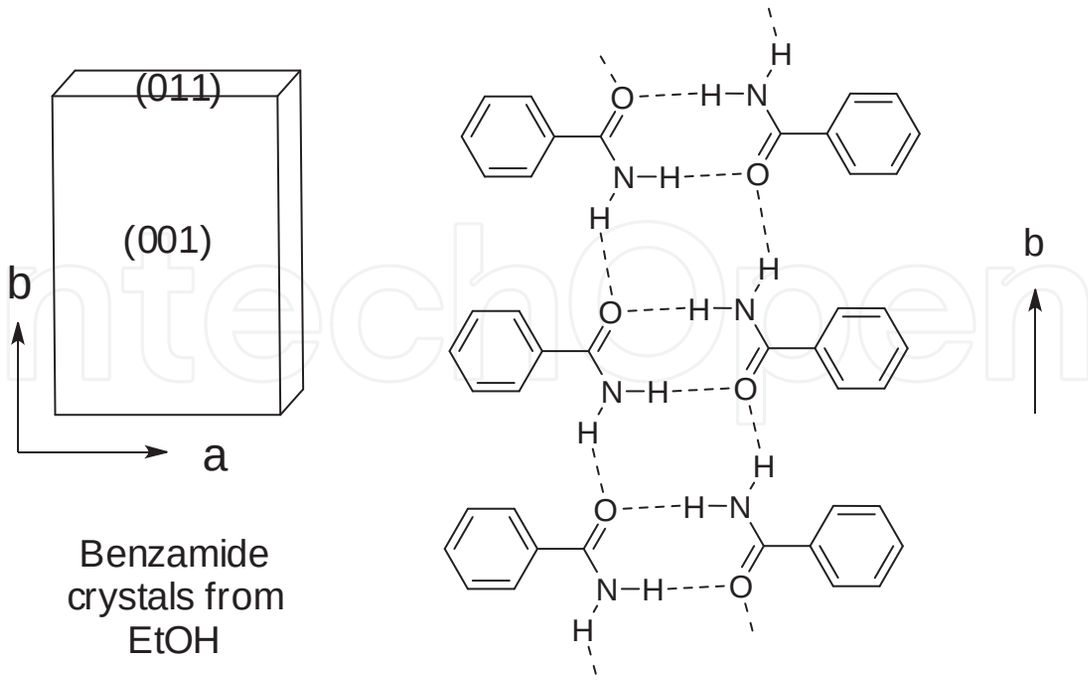


Figure 7. (Left) Typical habit of benzamide crystals grown from ethanol. (Right) 'Amide ladder' motif found in the crystal structure of benzamide.

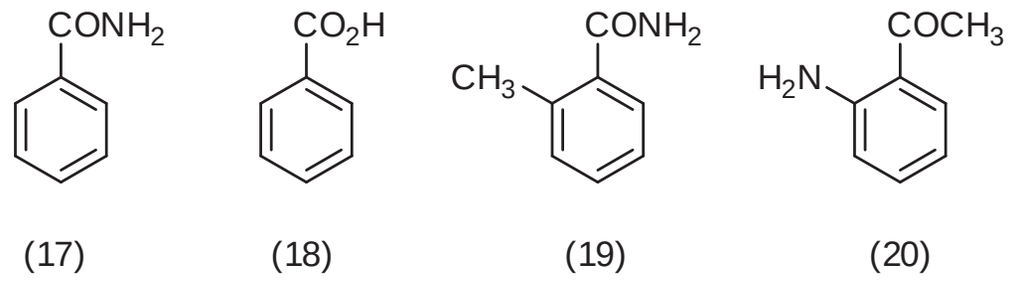


Figure 8. Molecular structure of benzamide (17) and impurities (18), (19) and (20).

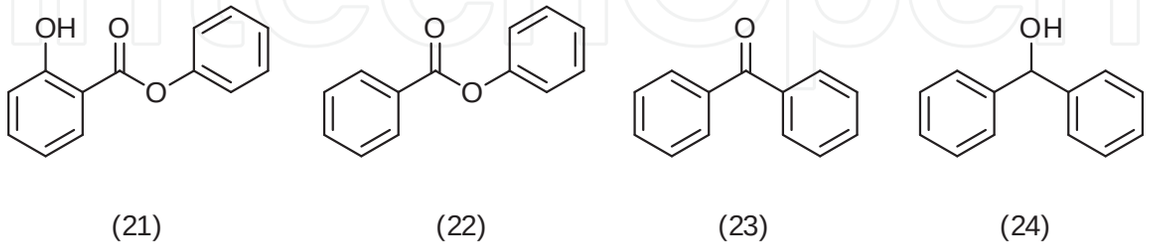


Figure 9. Molecular structures of phenyl salicylate (21), phenyl benzoate (22), benzophenone (23) and benzhydrol (24).

A challenging issue with regard to impurities in crystalline materials is the location of impurities within crystals, both with respect to the distribution of the impurities and the mode

of binding of the impurity 'guests' within the crystal 'host'. In manufacturing scale crystallisation, impurities are often adsorbed on crystal surfaces and can be removed by efficient washing. For example, a process for the crystallization of bisphenol A gave product which was 99.5% pure. It was found that the main source of impurities was from mother liquor adhering on crystal surfaces. The temperature stages of the crystallization protocol were changed to decrease the amount of fine crystals and increase the average crystal size. This allowed for improved separation of crystal product from the mother liquor, giving material of 99.8% purity. As the remaining impurities were likely to be trapped within the crystals, recrystallization was found to improve the quality of the bisphenol A product up to 99.99% [10]. Impurities which are not removable by washing may be located within the crystal and may be interacting with some aspect of the crystal lattice. X-Ray diffraction methods average over the diffracting domains and so do not detect the presence of impurity molecules routinely. Relatively few studies have investigated the location and supramolecular binding of exogenous molecules within molecular crystals. One such example concerns the crystallisation of L-asparagine monohydrate from water. Other amino acids present as impurities in solution can be incorporated into L-asparagine monohydrate crystals but to differing extents and distributions. Careful sequential dissolution and analysis studies on individual L-asparagine monohydrate crystals showed that most amino acid impurities were largely located on the outer or surface layers of the crystals. However, L-aspartic acid was found to be incorporated into L-asparagine monohydrate crystals in significant quantities (> 10%) and to be distributed relatively uniformly throughout the crystal, indicating a possible systematic substitution of L-aspartic acid molecules for L-asparagine molecules within the L-asparagine monohydrate crystals [11]. This possibility was confirmed by neutron diffraction studies of deuterated L-asparagine monohydrate crystals grown in the presence of deuterated aspartic acid, which showed a reduction in symmetry from $P2_12_12_1$ for L-asparagine monohydrate crystals to $P2_1$ for crystals grown with aspartic acid impurity, due to systematic substitution of aspartic acids molecules for aspargine molecules at specific sites in the crystal lattice [12].

In the course of studies on the crystallisation and morphology of phenacetin (26) [13], we observed a significant impurity arising with one of the main routes for preparing this compound, involving many of the issues encountered in the literature examples outlined above. Further investigation of this involved aspects such as the origin of impurities in the process chemistry, retention or rejection of specific impurities, the removal of impurities by washing and/or recrystallisation, and the supramolecular interactions between host crystals and retained impurities. These issues are described in the following section. Phenacetin has proved to be a useful compound for the study of crystallisation issues, as it is a relatively simple molecule but, as a former drug substance, of sufficient pharmaceutical relevance to be a worthwhile model.

2. Results and discussion

Phenacetin (4-ethyloxyacetanilide) (26) is a close analogue of paracetamol (acetaminophen or 4-hydroxyacetanilide) (27). Phenacetin was used as an analgesic and anti-pyretic drug before

http://dx.doi.org/10.5772/59715

being withdrawn due to nephrotoxicity [14]. Processes for the large scale manufacture for phenacetin have been described, in particular by the acetylation of *para*-phenetidine (4-ethyloxyaniline) (25) [15]. An essential part of these processes is the isolation of the phenacetin product as a crystalline precipitate of sufficient purity and crystal size distribution to meet pharmacopoeial requirements. For example, carrying out of the acetylation at temperatures over 100 °C in high boiling aromatic hydrocarbons, followed by cooling to under 10 °C with seeding, gives large scale batches of phenacetin of pharmacopoeial quality [16]. Alternative routes to phenacetin include the *O*-ethylation of paracetamol (27) which can be a more convenient process on a laboratory scale [17]. Both of these routes are summarised in Figure 10. Both routes give phenacetin as a crystalline product which, if required, can be further recrystallised to improve purity or particle properties.

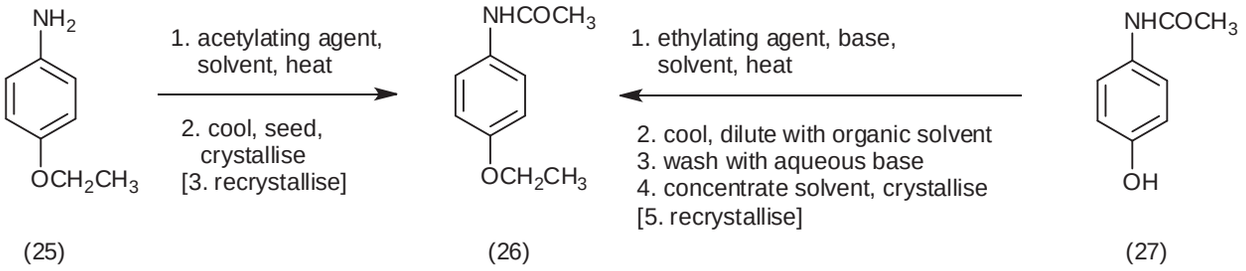
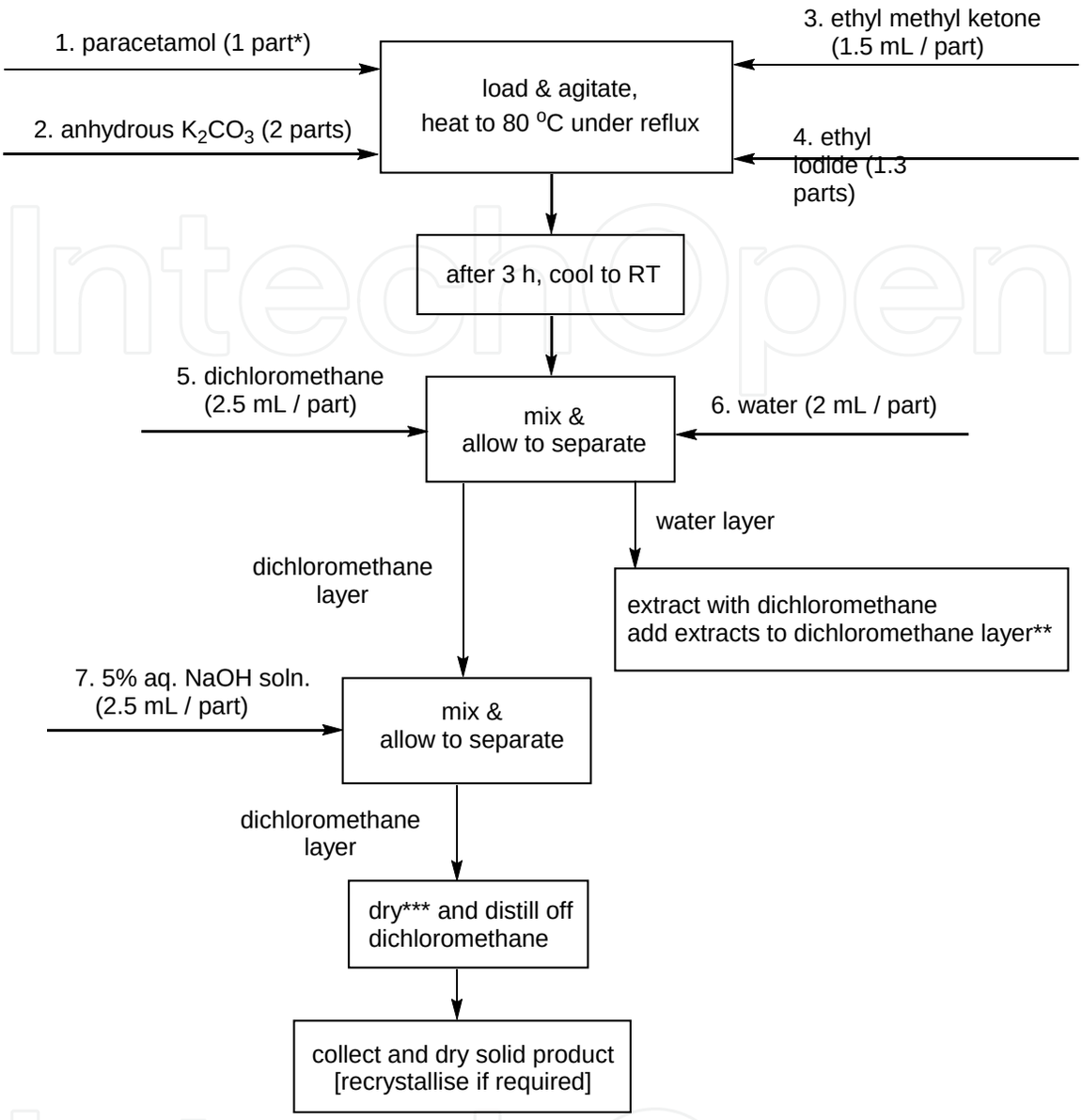


Figure 10. Summary of processes for the preparation of phenacetin (26) from *para*-phenetidine (25) or paracetamol (27).

Both routes summarised in Figure 10 were studied by us as part of an investigation into the phase, morphology, size distribution and purity of phenacetin batches obtained by various routes and using various crystallisation regimes [13]. For the reasons discussed in the Introduction, impurities, their origin in the process chemistry and their persistence in crystallised and recrystallised material, was a subject of particular importance in this investigation. Impurity issues were not found to be particularly significant in the acetylation route to phenacetin. However, we did find significant impurities arising from the ethylation route, which were subject to further investigation.

Figure 11 shows a block flow diagram for the ethylation process. This is an adaptation of the procedure described by Volker *et al* [17]. The reagents were charged to the reaction vessel in the order given and the mixture heated to the boiling point of ethyl methyl ketone with agitation. After three hours, the solution was allowed to cool, diluted with dichoromethane and washed with water to remove potassium iodide by-product. The final product yield could be improved marginally by extraction of the aqueous wash with dichloromethane and addition of the extracts to the main dichloromethane solution. This was washed with aqueous sodium hydroxide to remove unreacted paracetamol. The dichloromethane solution was dried to remove water dissolved in the dichloromethane, either by washing with brine or using a solid drying agent. Finally, the dichloromethane solvent was removed by distillation and the solid phenacetin product isolated and dried. Yields of product at this stage were typically 70-90%. The material can be subsequently recrystallised to improve purity or control particle properties.



*Relative quantities of reagents and solvent (parts) are based on molar equivalents.

**Extraction of the water washing to improve yield is optional.

***Final dichloromethane solution can be dried prior to removal of solvent by washing (with brine) or using a solid drying agent ($MgSO_4$) followed by filtration.

Figure 11. Block flow diagram for the synthesis of phenacetin (26) using the ethylation of paracetamol (27) process.

The phenacetin product was confirmed by ^{1}H NMR and IR spectroscopy (see the Experimental Methods section for details). DSC analysis of samples showed a single thermal event corresponding to melting with an on-set at 133 °C, agreeing with the literature value of 133.5 to 135.5 °C [18]. PXRD analysis (Figure 12) showed excellent correspondence with the theoretical pattern generated from the CIF file for the phenacetin structure recorded by Hansen et al [19] (CSD refcode PYRAZB21), which is a more recently determined structure than that reported

http://dx.doi.org/10.5772/59715

by Patel et al [20]; essentially showing that the phenacetin product is the expected crystal form, namely a monoclinic $P2_1/c$ structure with $Z = 4$. The initially obtained phenacetin solid could be recrystallised from a variety of solvents. Dichloromethane, ethanol, water and acetonitrile were found to be the most useful, giving yields of 70-90% of recrystallised phenacetin. PXRD and DSC analysis of the recrystallised material gave data which were essentially identical to those obtained from the initially obtained solid. Figure 13 shows examples of the DSC data, showing melting points lying within the range 134-139 °C. Micrographs showing typical morphologies of phenacetin crystals obtained from these solvents are shown in Figure 14. Those obtained from dichloromethane were typically block-like prisms, needles from ethanol, flaky plates from water and elongated prisms from acetonitrile.

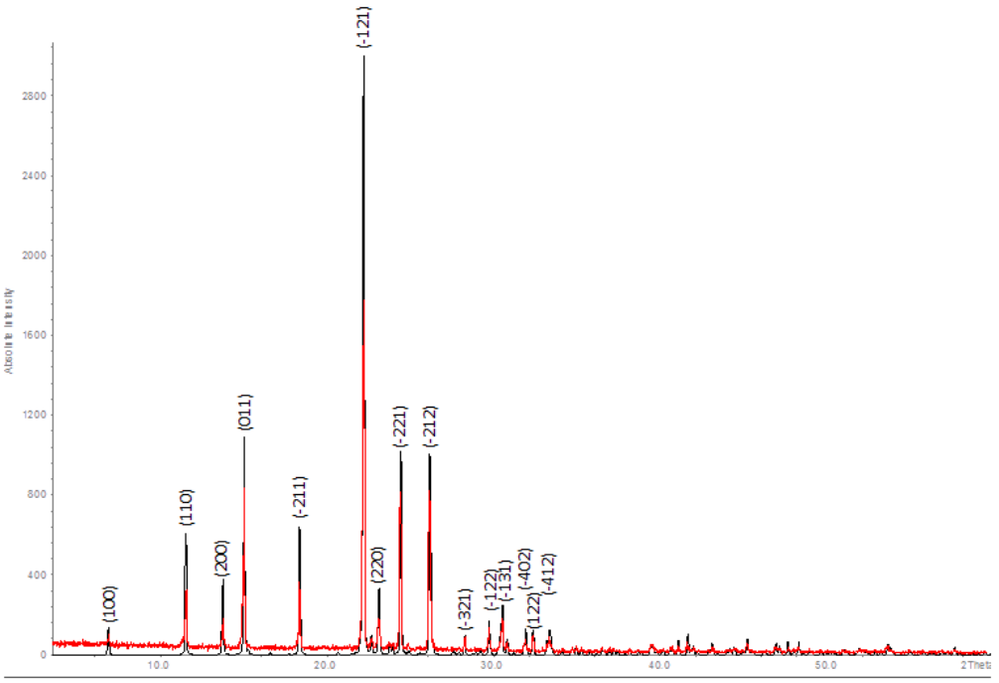


Figure 12. PXRD pattern of (in red) phenacetin (26) product and (in black) the theoretical pattern generated from PYRAZB21 [19] including indices of the diffraction peaks.

The purity of the phenacetin batches was determined by HPLC. No residual paracetamol starting material was detected. However, an unknown impurity was observed, eluting after paracetamol and before phenacetin. The intensity of the impurity peak suggested its presence in approximately 1% quantity, assuming a structural similarity to phenacetin. Likely candidates for this impurity were compounds (28) or (29) in Figure 15, arising from competing *N*- or *O*-ethylation at the amide groups, or di-ethylated analogues (30) or (31). To confirm or reject these compounds as the unknown impurity, it was necessary to independently synthesise both the amide-ethylated (28 or 29) and di-ethylated (30 or 31) derivatives. These were prepared *via* the route shown in Figure 16, which involved an initial protective *O*-benzylation of paracetamol, followed by ethylation of the amide group. Under the ethylation conditions (potassium *tert*-butoxide base in dry THF, ethyl iodide and sodium iodide), the *O*-benzyl group was also

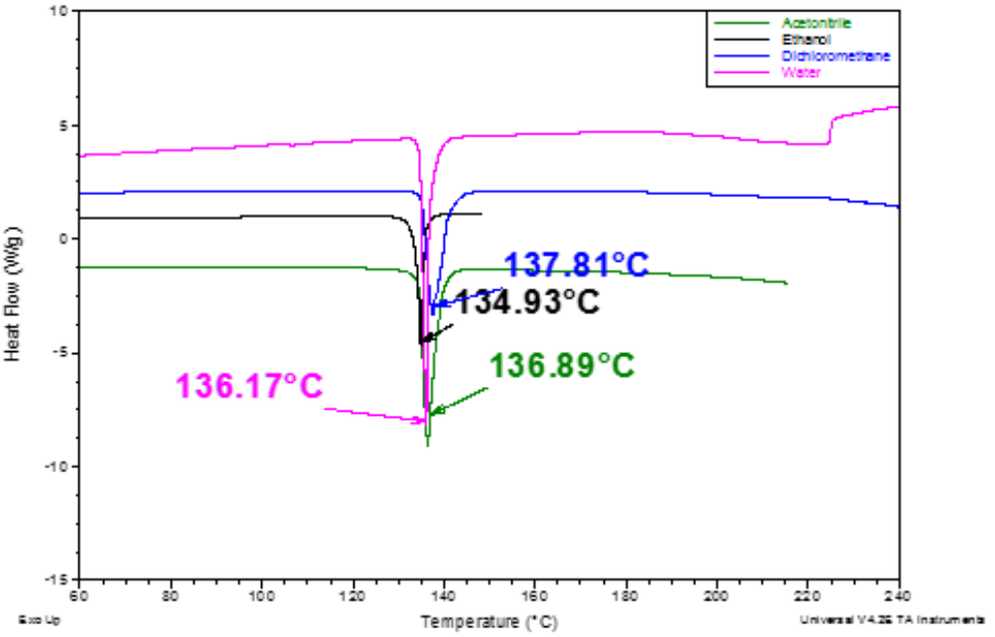


Figure 13. DSC data of phenacetin recrystallised from water (magenta curve), dichloromethane (blue curve), ethanol (black curve) and acetonitrile (green curve).



Figure 14. Optical micrograph of phenacetin recrystallised from (top left) dichloromethane, (top right) ethanol, (bottom left) water and (bottom right) acetonitrile.

http://dx.doi.org/10.5772/59715

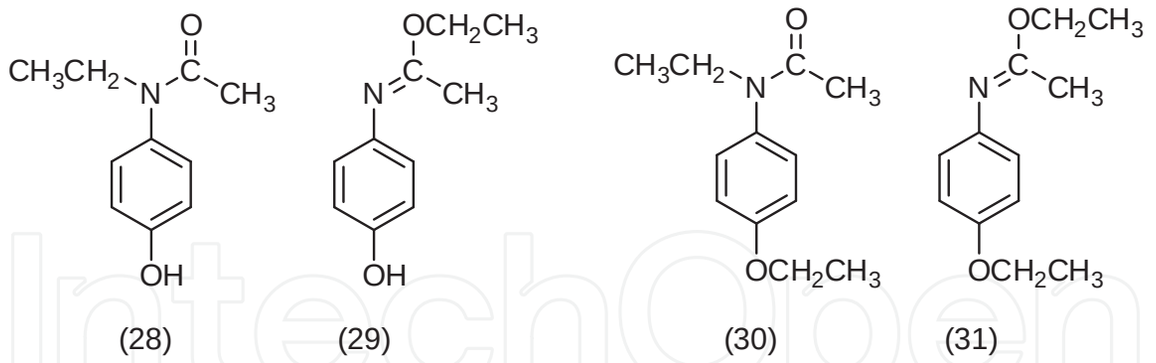


Figure 15. Possible impurity products arising from the preparation of phenacetin by ethylation of paracetamol.

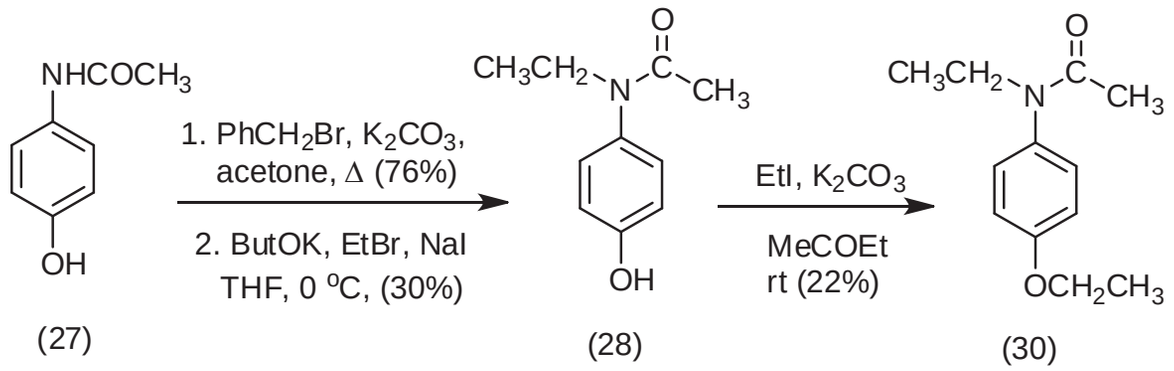


Figure 16. Preparation of *N*-ethyl derivative (28) and *N,O*-diethylated derivative (30).

removed, giving the amide-ethylated derivative (28) without need for a specific debenzylation step. This is likely to be a consequence of iodide induced cleavage of the benzylic C-O bond. A further *O*-ethylation step gave the diethylated derivative (30). In both derivatives, ethylation at the amide group was found to occur on nitrogen rather than oxygen, i.e. compounds (29) and (31) were not observed.

HPLC of samples of phenacetin containing the unknown impurity, of samples of *N*-ethyl derivative (28), and of samples of phenacetin containing the unknown impurity also spiked with *N*-ethyl derivative (28) (Figure 17), provide strong evidence that the unknown impurity was *N*-ethyl derivative (28), i.e. *N*-ethylparacetamol. This is a perfectly reasonable finding in terms of the process chemistry, i.e. in reaction of paracetamol (27) with ethyl iodide and potassium carbonate in ethyl methyl ketone, *O*-ethylation to give phenacetin (26) is the major process while approximately 1% of the batch undergoes competing amide *N*-ethylation to give impurity (28). Impurity (28) was not detected in recrystallised samples of phenacetin, i.e. a single recrystallization step was sufficient to remove the impurity.

Of particular interest was to examine the impact of *N*-ethyl impurity (28) on the crystallisation of phenacetin (26) in terms of the crystallisation process, the resulting crystal form and the resulting crystal morphology. These studies were carried out on samples on phenacetin which

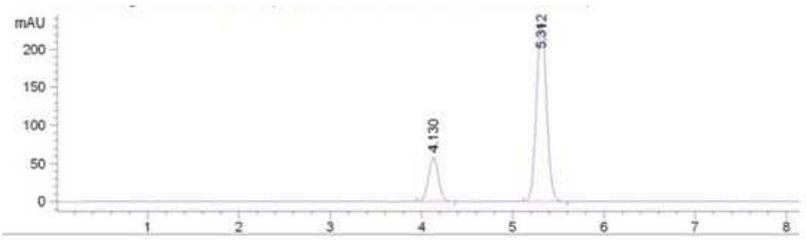


Figure 17. HPLC of a phenacetin sample containing the unknown process impurity spiked with *N*-ethylparacetamol (28). Phenacetin elutes at 5.312 min, while the unknown impurity and *N*-ethylparacetamol (28) co-elute at 4.130 min.

were shown to be pure by HPLC. In addition to investigating the impact of impurity (28), the effect of the paracetamol starting material was also examined.

Addition of either paracetamol (27) or *N*-ethylparacetamol (28) as a 1% impurity was found to have no detectible effect on the metastable zone width (MSZW) of crystallisation of phenacetin from ethanol. i.e. the equilibrium solubility and metastable solubility curves were not significantly changed (Figure 18). Addition of paracetamol at levels as high as 10% impurity likewise gave rise to no discernible change in the MSZW. Likewise, PXRD data of samples of phenacetin recrystallised in the presence of 1% of either paracetamol (27) or *N*-ethylparacetamol (28) were all identical to those previously obtained for phenacetin (e.g. as in Figure 12) implying that no change was observed in the phenacetin crystal form due to the presence of the impurities, at least that would be detectible by PXRD. The same finding was observed from crystals grown in the presence of 10% paracetamol impurity. Inclusion of paracetamol (27) or *N*-ethylparacetamol (28) impurities in phenacetin (27) crystallisations from ethanol had a significant impact on the morphologies of the resulting phenacetin crystals. Crystallisation of pure phenacetin from ethanol give acicular needles (Figure 19). Inclusion of the impurities resulted in smaller and less elongated crystals, as shown in Figure 20 for 1% and 10% paracetamol impurity. While the phenacetin crystals grown in the presence of 1% impurity retained their essential morphology with a more prismatic, rather than acicular, habit, the crystals obtained in the presence of 10% impurity were agglomerated particles which lacked well developed faces.

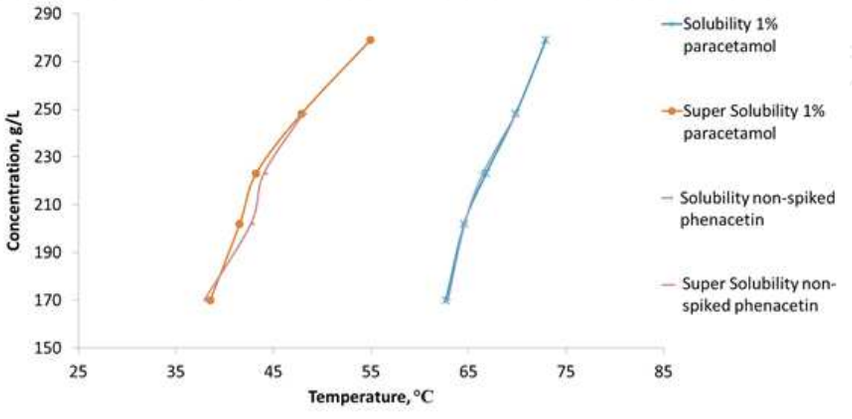


Figure 18. MSZW of pure phenacetin compared with samples of paracetamol-spiked phenacetin.

http://dx.doi.org/10.5772/59715



Figure 19. Acicular crystals of pure phenacetin grown from ethanol.

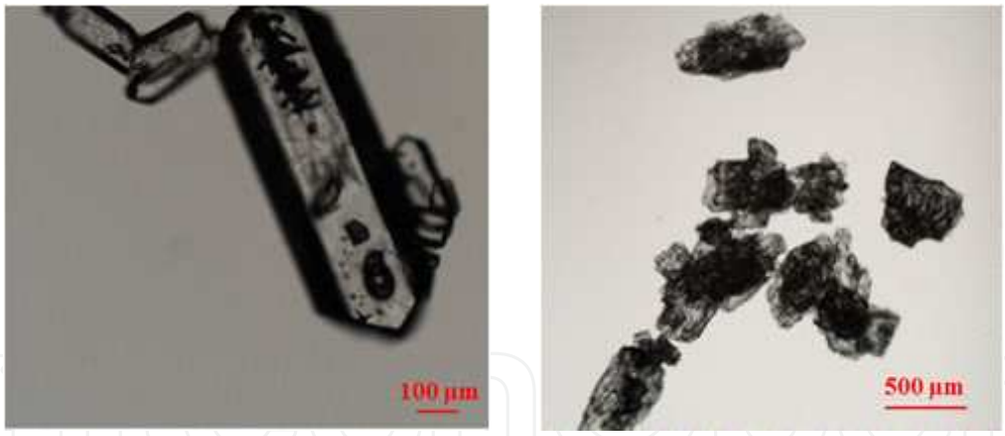


Figure 20. Phenacetin crystals grown from ethanol in the presence of (left) 1% w/w paracetamol and (right) 10% w/w paracetamol impurity.

Pure phenacetin crystallised from ethanol grows as acicular prisms as shown in Figure 19. Figure 21 shows one of these crystals mounted on the goniometer of an X-ray diffractometer; sufficient diffraction data has been collected to allow the crystallographic directions to be determined. This shows that the needles are elongated along the *a* crystallographic direction. Figure 22 shows the crystal structure of phenacetin [19] viewed both along the *b* and *c* axes. These images show that the ethyloxy and acetyl groups of the phenacetin molecules are oriented along the *a* crystallographic direction. The most important supramolecular motif

present in the structure is a so-called amide C(4) chain, i.e. a repeated hydrogen bond between secondary amide hydrogens and carbonyl oxygen atoms (N-H•••O=C-N-H•••O=C). As the motif is a hydrogen bonding chain with four atoms in the repeat unit, it is designated C(4) according to Etter's notation [21]. The C(4) chain is lying in the *bc* plane. In crystallisation of phenacetin from ethanol, hydrogen bonding by the hydroxyl group of ethanol to surface carbonyls or N-H groups are likely to reduce the rate of growth in the *b* and *c* crystallographic directions, giving rise to the needles elongated along *a*, as seen in Figure 19. Figure 23 shows a phenacetin crystal grown from ethanol containing 1% paracetamol. The crystal is typical of those grown in the presence of 1% paracetamol impurity, i.e. it is a reasonably well formed elongated prism, but not a needle. The direction of elongation is still the *a* crystallographic direction, i.e. the paracetamol impurity has had the greatest effect in the direction of most crystal growth for the pure crystals.

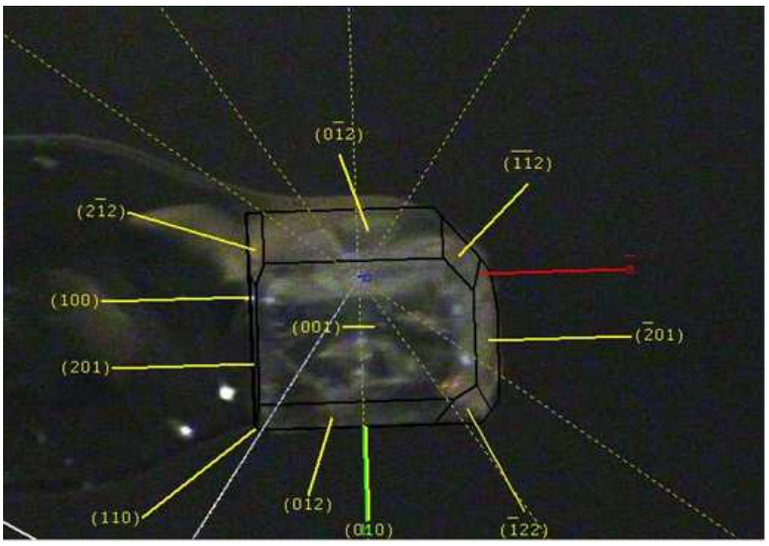


Figure 21. A crystal of pure phenacetin grown from ethanol mounted on the goniometer of an X-ray diffractometer and the directions of the crystallographic axes and indices of the main faces determined. Note that the crystal is a needle, similar to those shown in Figure 19, which has been cut to allow mounting onto the diffractometer. The cut is perpendicular to the *a* axis direction and has exposed a fresh (100) face.

As mentioned above, the initially formed phenacetin material found to have 1% of *N*-ethylparacetamol (28) present as an impurity, was not detected in recrystallised batches of phenacetin, i.e. it was removed by recrystallization. The staring material for a chemical process is always a candidate impurity, however, no residual paracetamol (27) starting material was detected in the initially crystallised phenacetin material. Part of the phenacetin by ethylation of paracetamol process involves an aqueous base extraction intended to remove unreacted paracetamol (addition 7 in Figure 11). While this step would be expected to minimise the amount of paracetamol starting material present, some residual paracetamol impurity could still be a possibility requiring investigation. As a phenol, *N*-ethylparacetamol (28) should also be to some extent extractible with an aqueous base wash, although less so than paracetamol, which is more hydrophilic. Nonetheless, *N*-ethylparacemol (28) was found to be present as an

http://dx.doi.org/10.5772/59715

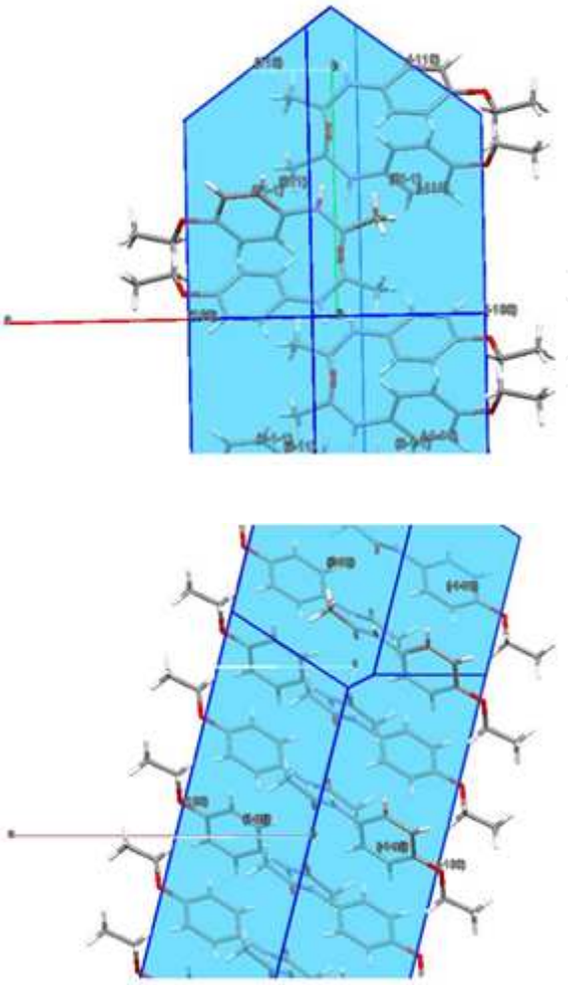


Figure 22. Images of the crystal structure of phenacetin generated from the structure reported by Hansen et al [19], viewed (top) in the *ab* plane along *c* (which corresponds to the orientation shown in Figure 21) and (bottom) in *ac* plane along *b*.

impurity. However while impurity (28) could be removed by recrystallization, spiking experiments with paracetamol found that this was a more persistent impurity. Recrystallisation of phenacetin from ethanol in the presence of 1% or 10% w/w of added paracetamol gave phenacetin crystals containing, respectively 0.16% and 6.0% paracetamol impurity by HPLC. Growing phenacetin crystals therefore appear to have differing affinity for *N*-ethylparacetamol and paracetamol as impurities for inclusion, with the former being generally excluded while the latter is incorporated to a considerable extent. A second recrystallisation was often necessary to fully remove paracetamol impurity.

The relative preferential exclusion of *N*-ethylparacetamol and inclusion of paracetamol can be rationalised by consideration of the crystal structure of phenacetin. As mentioned above, the most significant supramolecular motif present in the structure is an amide C(4) chain. Only primary or secondary amides, such as phenacetin, can participate in amide C(4) chains. Tertiary amides, such as *N*-ethylparacetamol, can 'end-cap' such chains by accepting a hydrogen bond at the amide carbonyl oxygen; however they cannot continue the chain. Hence,

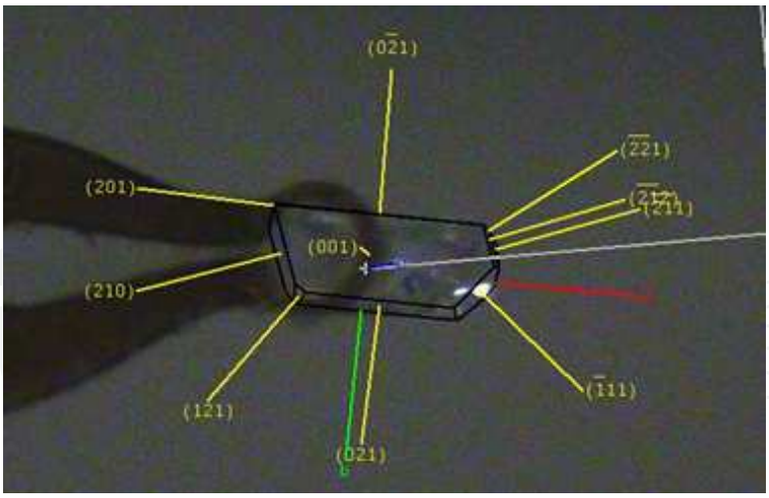


Figure 23. A crystal of phenacetin grown from ethanol containing 1% paracetamol, mounted on the goniometer of an X-ray diffractometer and the directions of the crystallographic axes and indices of the main faces determined. Note that the crystal is intact as grown and has not been cut.

inclusion of *N*-ethylparacetamol molecules results in discontinuation of the phenacetin C(4) chain and is incompatible with the bulk crystal structure. By comparison, paracetamol, as a secondary amide, can participate in an amide C(4) motif. The key point of difference in the molecular structures of phenacetin and paracetamol is the replacement of the ethyloxy group of phenacetin by a hydroxyl group in paracetamol. In the crystal structure of phenacetin, the ethyloxy groups occupy hydrophobic regions as shown in Figure 24. The replacement of a small number of ethyl groups by hydrogen atoms in these regions seems reasonable. Therefore, it is feasible that a small number of paracetamol molecules could take the place of phenacetin molecules in phenacetin crystals, while *N*-ethylparacetamol molecules could not easily be accommodated within continuous phenacetin crystallites. These proposed supramolecular interactions are shown schematically in Figure 25.

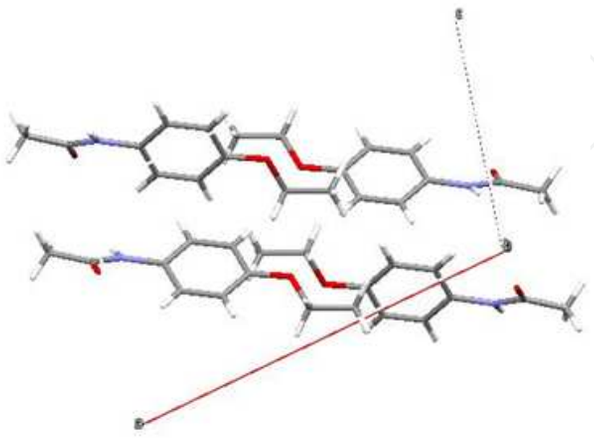


Figure 24. View of the crystal structure of phenacetin [19] along the *b* crystallographic axis, showing the packing of the phenacetin ethyloxy groups.

http://dx.doi.org/10.5772/59715

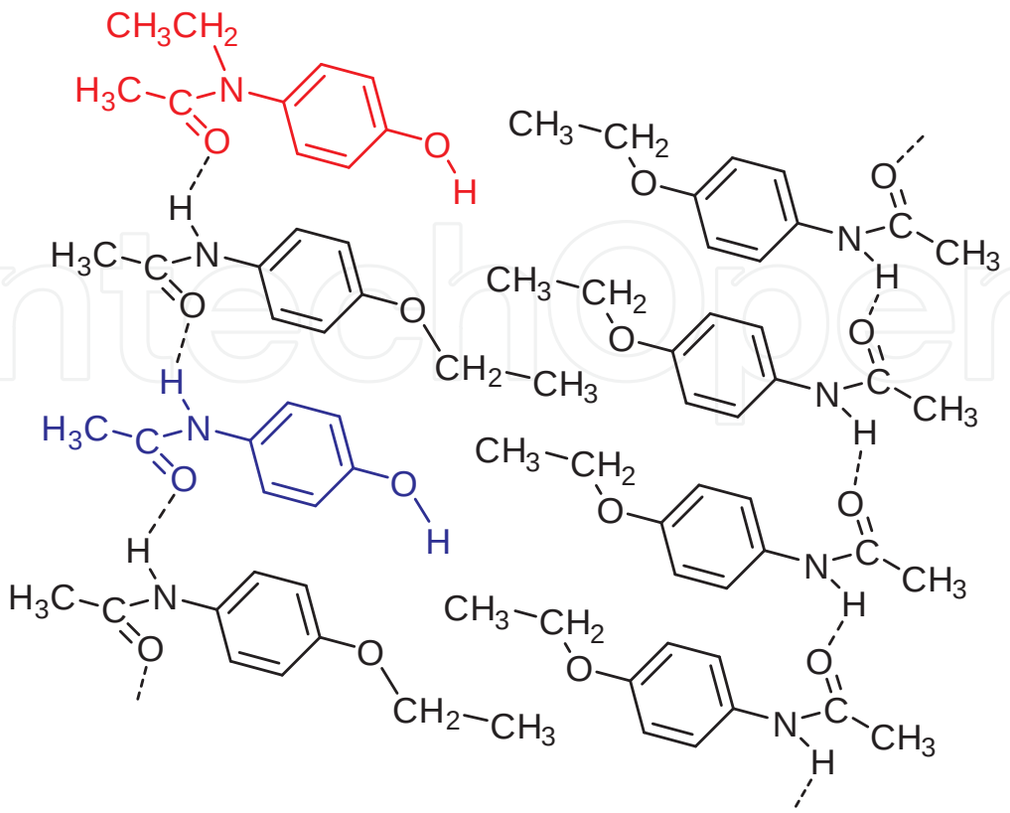


Figure 25. Schematic representation of the molecular packing in the crystal structure of phenacetin incorporating *N*-ethylparacetamol (red) and paracetamol (blue) molecules. The phenacetin molecules are linked by an amide C(4) hydrogen bonding chain [21] shown using dashed lines. The ethyloxy groups of the phenacetin molecules occupy a hydrophobic region of the structure. The *N*-ethylphenacetin molecule (red) can 'end-cap', but not continue the C(4) chain, while the paracetamol molecules (blue) can fully participate in the C(4) chain. The hydroxyl groups of both paracetamol or *N*-ethylparacetamol could feasibly sit within the hydrophobic region containing the ethyloxy groups.

The proposal discussed above and illustrated in Figure 25 suggests the possibility of substantial and possibly systematic inclusion of paracetamol molecules in phenacetin crystals. To investigate this possibility, a series of successive dissolution experiments were carried out on individual phenacetin crystals, in a similar manner to those described by Addadi et al in the investigation of L-asparagine monohydrate / L-aspartic acid host / guest systems [11, 12]. The crystals for this study were grown from ethanol solutions of phenacetin containing either 5%, 10% or 15% (w/w phenacetin) of added paracetamol. Examples of these crystals are shown in Figure 26. These crystals were then dissolved in methanol-water (40:60) in three successive dissolutions, i.e. approximately one third of the crystal dissolved in the first dissolution step, another third in the second and the remainder of the crystal dissolved in the final step. After each dissolution, the resulting solution was analysed by HPLC for phenacetin and paracetamol content. The data obtained are given in Table 1. These data show that the paracetamol content of the crystals is considerably greater in the outermost portions of the crystals which are dissolved in the first dissolution step. This may include paracetamol which has been deposited on crystal surfaces as well as paracetamol which has been included within the crystals. Importantly, paracetamol is still present in the second and innermost portions of the crystals.

Therefore, the paracetamol impurity is being incorporated into the phenacetin crystals at all stages of crystal growth, and especially in the later stages of growth. Possibly, increased uptake of paracetamol impurity is connected to a significant reduction and termination of crystal growth.

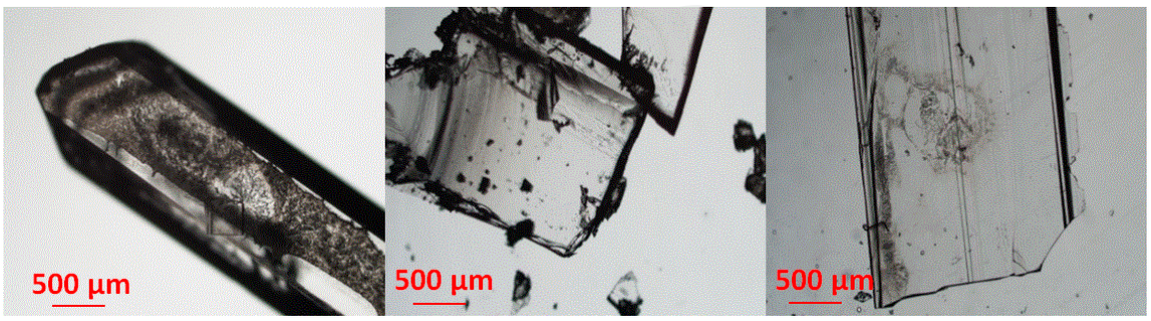


Figure 26. Examples of phenacetin crystals grown from ethanol containing (left to right) 5%, 10% and 15% (w/w phenacetin) added paracetamol.

Dissolution Step	% Impurity added	% Paracetamol	% Phenactin
1st	5	14.16	85.47
2nd	5	1.57	98.32
3rd	5	0.71	99.14
1st	10	7.88	91.59
2nd	10	0.40	99.38
3rd	10	0.00	99.53
1st	15	5.42	94.48
2nd	15	2.83	97.06
3rd	15	1.87	98.09

Table 1. Three stage dissolution of individual phenacetin crystals grown from ethanol containing paracetamol; HPLC analysis of solution from each dissolution step.

The above finding raises the possibility that phenacetin molecules may be systematically replaceable by paracetamol molecules to some extent in the crystal structure of phenacetin. If this was to be the case, it should be possible to obtain phenacetin / paracetamol co-crystals. This possibility was investigated by attempting co-crystallisation of 1:1 and 2:1 phenacetin : paracetamol mixtures, both from solution and by neat grinding. PXRD of the resulting solids (Figure 27) were all very similar to those for phenacetin with some additional peaks, for example at 2θ = 12.0° and 23.2°. This does not confirm formation of a co-crystal.

http://dx.doi.org/10.5772/59715

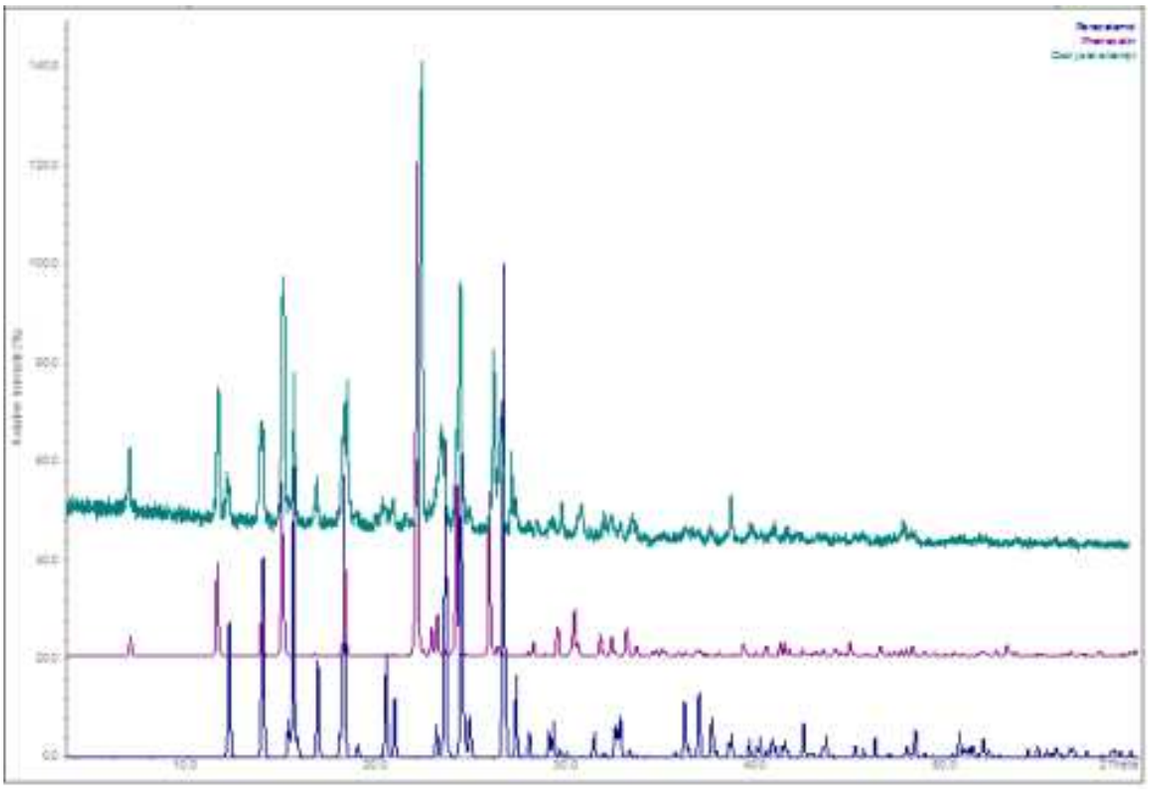


Figure 27. PXRD patterns for (top), material obtained by attempted cocrystallisation of phenacetin and paracetamol (1:1 neat grinding); (middle) theoretical pattern for phenacetin generated from PYRAZB21 [19]; (bottom) theoretical pattern for monoclinic paracetamol [22].

3. Conclusions

The preparation of phenacetin (26) by *O*-ethylation of paracetamol (27) has been investigated as a study into the generation of process impurities and their impact on crystallisation and recrystallisation of crystalline solid products. In the *O*-ethylation of paracetamol, paracetamol is reacted with ethyl iodide in the presence of potassium carbonate base in ethyl methyl ketone solvent heated to 80 °C. After cooling to room temperature, the reaction mixture is dissolved in dichloromethane and washed with water, aqueous sodium hydroxide, dried and the solvents removed to give a crystalline solid. This can be recrystallised from solvents including ethanol, acetonitrile, water or dichloromethane, giving rise to crystals as, respectively, needles, prisms, plates or thin plates. Yields from this process were in the range of 70-90%, providing material consistent with the structure of phenacetin by ^{1}H NMR and IR spectroscopy. The crystal form of all phenacetin batches obtained was consistent with the structure reported by Hansen et al [19] and previously by Patel et al [20] even when analysed by both PXRD and DSC.

HPLC analysis of the initially obtained phenacetin solid showed the presence of a compound not corresponding to phenacetin or the starting material. Likely candidates for this impurity

were compound (28), formed by competing ethylation at the amide rather than the phenolic site of phenacetin, or compound (30) formed by diethylation. Independent synthesis of both compounds followed by HPLC comparison of these with the impurity confirmed that the impurity was compound (28), i.e. *N*-ethylparacetamol, present in, typically, 0.9% quantities in initially obtained phenacetin solid. Impurity (28) was not detected in any samples of recrystallised phenacetin, i.e. the impurity was removed by recrystallisation.

Both *N*-ethylparacetamol (28) and the starting material in the process, paracetamol (27), were investigated in spiking experiments at a 1% level for their impact on the generation of supersaturation and on crystal form and morphology in crystallisations of phenacetin from ethanol. Paracetamol (27) was also investigated at a 10% impurity level. Neither impurity was found to have any effect on MSZW, or on crystal form. However, significant changes were observed on crystal morphology, which transforms from needles for pure phenacetin, to smaller elongated prisms with 1% impurities and to polycrystalline agglomerates with 10% paracetamol. Orientation of crystals on an X-ray diffractometer show that the needles were elongated along the *a* crystallographic axis and that the shorter prisms were also elongated in the *a* direction. The ethyloxy and acetamido groups of phenacetin are directed along the *a* direction, while an amide C(4) chain lies in the *bc* plane. In crystallisations of phenacetin from ethanol, growth in the *bc* directions is hence impeded by hydrogen bonding of the solvent, leaving the *a* direction as the fastest growing direction. As would be expected, the impurities have the most impact in the fastest growing direction, reducing the extent of growth in that direction to change the crystal habit from needles, to small elongated prisms, to polycrystalline agglomerates.

HPLC analysis of samples of phenacetin crystallised in the presence of quantities of paracetamol (27) or *N*-ethylparacetamol (28) and then recrystallised showed that whereas *N*-ethylparacetamol (28) can be effectively removed by recrystallisation, paracetamol (27) when present as an impurity is incorporated into phenacetin crystals by a greater extent and is also retained within the crystals to a significant extent even after recrystallisation. Phenacetin and paracetamol are both secondary amides and so can participate in amide hydrogen bonded C(4) chains. *N*-Ethylparacetamol (28), as a tertiary amide, cannot participate in an amide C(4) chain, but can terminate such a chain. Hence it is feasible that a paracetamol impurity molecule can substitute for a phenacetin molecule in the bulk of the crystal lattice in a manner not possible with *N*-ethylparacetamol. *N*-Ethylparacetamol impurity can add to phenacetin crystals at the ends of amide chains, or by other supramolecular interactions, but cannot be easily accommodated within the crystal lattice and so is incorporated to a lesser extent and is easily removed by recrystallisation. This proposal offers a rationale for the respective retention and rejection of paracetamol and *N*-ethylparacetamol by phenacetin crystals, which is summarised schematically in Figure 25. This model requires the phenolic hydrogen of paracetamol (or *N*-ethylparacetamol) to reside within a region dominated by phenacetin ethyl groups, which is not unreasonable.

The above proposal raises the possibility that paracetamol molecules could systematically substitute for phenacetin molecules in phenacetin crystals, in a manner best exemplified by the case of L-aspartic acid in L-aspargine monohydrate described by Addadi et al [11, 12]. To

http://dx.doi.org/10.5772/59715

examine this possibility, we carried out a series of sequential dissolution experiments on single crystals of phenacetin grown in the presence of 5 to 15% paracetamol impurity and analysed the resulting solution for phenacetin and paracetamol. The results, given in Table 1, show that the majority of the incorporated impurity resides in the outer layers or surface of the crystals, although detectible quantities of impurity can be found throughout the crystal. This suggests that paracetamol incorporation into phenacetin crystals is occurring at all stages of crystal growth, but becomes most prevalent in the later stage of growth and may be associated with the termination of crystal growth. This implies that systematic substitution of paracetamol for phenacetin molecules in the crystal lattice is probably not occurring, but that solid solutions of paracetamol in phenacetin may be occurring. The possibility of phenacetin / paracetamol cocrystallisation was examined but conclusive formation of cocrystals was not obtained.

The phenacetin by ethylation of paracetamol system has produced some instances of impurity behaviour which is highly characteristic of the synthesis and crystallisation of molecular organic compounds as pharmaceuticals or fine chemicals. A process impurity, *N*-ethylparacetamol, does form and is present in the initially precipitated crystals, but is easily removed by recrystallisation as a likely consequence of its limited ability to engage with the supramolecular packing of the phenacetin crystal structure. By contrast, the starting material, paracetamol, is well incorporated and retained within phenacetin crystals, quite likely as a consequence of its compatibility with the crystal structure of phenacetin. The paracetamol impurity in phenacetin crystal system is therefore a good model on which to investigate methods for removing recalcitrant structurally-related impurities. Selective co-crystallisation is one method which has received recent attention [23, 24] and which could be vary amenable to this system. Many co-crystals of paracetamol have been prepared. What is required in this case is paracetamol co-crystals in which the phenolic hydroxyl group of paracetamol is engaged in a specific supramolecular motif. This allows a key point of differentiation from phenacetin, in which the phenolic hydroxyl group is replaced by an ethyloxy group. *N*-Methylmorpholine, pyrimidine [25] and trimethylglycine [26] form such co-crystals with paracetamol. In further studies on this system, these compounds will be investigated as putative selective paracetamol impurity removers.

4. Experimental methods

All chemicals were purchased from Sigma-Aldrich. ^{1}H NMR spectra were recorded on either a Bruker AVANCE 300 MHz spectrometer or a Bruker AVANCE 400 MHz spectrometer. Chemical shift values are expressed as parts per million (ppm). High resolution mass spectra were recorded on a Waters LCT Premier LC-MS instrument in electrospray ionisation (ESI) positive mode using 50 % acetonitrile / water containing 0.1 % formic acid as eluent; samples were made up in acetonitrile.

Preparation of phenacetin (26) by ethylation of paracetamol (27), typical procedure. A mixture of 1.51 g (10 mmol) of paracetamol (27), 2.76 g (20 mmol) of anhydrous potassium carbonate, 15 mL of methyl ethyl ketone and 2.0 g (13 mmol) of ethyl iodide was heated to reflux for 3 hours

with magnetic or mechanical stiring. The solution was allowed to cool to room temperature before addition of 25 mL of dichloromethane and washing with 20 mL of deionised water. The aqueous layer was extracted with 2 x 25 mL portions of dichloromethane which were combined with the dichloromethane layer, washed with 25 mL of 5% aq. sodium hydroxide solution before drying over $MgSO_4$ and concentration on the rotary evaporator. The material was further dried in air to give a white solid: 1.66 g, 93% yield; mp: 133-136 °C (lit. mp 133.5-135.4 °C [18]) IR (KBr disc) 3286 (N-H), 1660 (C=O), 1510, 1481 and 1245 (C-O) cm^{-1}. ^1H NMR (300MHz; $CDCl_3$) 1.40 (3H, t, $J_{H\text{-}H}$ = 6.9 Hz, $CH_2C\mathbf{H}_3$), 2.15 (3H, s, $COC\mathbf{H}_3$), 4.00 (2H, q $J_{H\text{-}H}$ = 6.9 Hz, $C\mathbf{H}_2CH_3$), 6.81-6.88 (2H, m, -Ar**H** x 2), 7.09 (1H, br s, NH), 7.34-7.40 (2H, m, Ar**H** x 2).

Differential Scanning Calorimetry (DSC) was carried out on a TGA Q1000 DSC with an RCS 40 cooling system using crimped aluminium pans at a variety of cooling rates between 2 to 10 °C/min.

Powder X-Ray Diffraction (PXRD) data was recorded on a Stoe Stadi MP diffractometer operating in transmission mode, with a tube voltage of 40 kV and current of 40 mA, using Cu $K\alpha_1$ monochromated radiation (1.5406 Å) and a gas-filled PSD detector. Diffraction was recorded over 5 to 60 °2θ in steps of 2 °/min. Samples were held between acetate foils and were not ground. Calculated patterns were generated from crystallographic information files using the THEO function on Stoe WinX^{POW} software with a pseudo-Voight profile shape and a gauss component of 0.8. Tables 2 and 3 give the calculated °2θ, *hkl* and intensity values for the calculated diffraction patterns for phenacetin and monoclinic paracetamol, calculated from PYRAZB21 [19] and HXACAN01 [22] respectively.

º2θ	*hkl*	I/I_{max} (%)
6.832	100	4.677
11.459	110	20.171
13.688	200	12.701
14.964	011	36.491
18.283	-211	21.346
22.119	-121	100
23.035	220	5.758
24.354	-221	0.012
26.088	-212	34.429
28.184	-321	3.304
29.647	-122	5.813
30.432	-131	8.592
31.852	-402	4.655
32.282	122	3.794
33.219	-412	2.392s

Table 2. Powder X-ray diffraction peaks (°2θ), diffracting plane indices (*hkl*) and relative intensities (I/I_{max}) for the calculated pattern for phenacetin based on the crystal structure reported by Hansen et al [19], CSD refcode PYRAZB21, calculated for X-rays of wavelength 1.5406 Å.

http://dx.doi.org/10.5772/59715

º2θ	*hkl*	I/I_{max} (%)
12.096	110	28.197
13.854	001	41.197
15.478	-201	59.166
16.769	011	20.322
18.140	-211	57.475
18.866	020	2.711
20.363	120	21.266
20.812	111	12.428
23.016	-311	6.563
23.482	021	64.893
24.330	220	83.339
24.821	310	0.292
26.561	121	100
27.209	-112	17.247
27.916	002	5.282
29.917	-411	7.444
31.330	221	5.179
32.702	-412	8.321
36.103	-511	11.289
36.853	330	13.205
37.559	202	6.217
38.565	-132	4.862
40.048	-431	0.275
42.373	430	0.662
43.553	013	4.524
46.130	241	4.354
48.245	-233	5.479
50.569	051	0.001

Table 3. Powder X-ray diffraction peaks (°2θ), diffracting plane indices (*hkl*) and relative intensities (I/I_{max}) for the calculated pattern for monoclinic paracetamol based on the crystal structure reported by Haisa et al [22], CSD refcode HXACAN01, calculated for X-rays of wavelength 1.5406 Å.

Recrystallisations: Samples of phenacetin (2) were dissolved in the minimum amount of boiling solvent required for dissolution. The solutions were allowed to cool to room temperature and

held isothermally with evaporation of solvent until solid material had formed. Crystals were isolated by filtration and dried under vacuum for 24 h.

Optical microscopy: Crystals were viewed using a Nikon Eclipse 50i POL Polarizing Microscope equipped with a Nikon DS-Fi1 CCD camera.

HPLC was carried out using an Agilent 1100 series HPLC, equipped with quaternary pump and degasser, and a YMC-Pack ODSA column (250 x 4.6 mm, 5μm). The column was eluted with a phosphate buffer at a flow rate of 1 mL/min and injection volume of 5 μL. The oven temperature was maintained at 20°C. The detector was initially set at 350 nm. The elution was isocratic, using methanol-water (60:40 v/v). Under these conditions, paracetamol eluted at 3.0 min and phenacetin at 5.3 min. Calibration curves were constructed by injection of different volumes of a stock solution (1 mg/mL) of compound (phenacetin or paracetamol) and plotting the ratios of the peak heights against the quantities injected. Calibration curves for phenacetin and paracetamol had R^2 values of 0.9993 and 0.9985 respectively.

Synthesis of candidate impurity compounds (28) and (30)

Paracetamol (27) (1.00 g, 6.6 mmol) and potassium carbonate (1.82 g, 13.2 mmol) were dissolved in 40 mL of acetone. Benzyl bromide (0.66 mL, 6.6 mmol) was added, and the solution was heated under reflux for 72 h. After this time, one further equivalent of potassium carbonate (1.82 g, 13.2 mmol) and 0.5 equivalents of benzyl bromide (0.32 mL, 3.3 mmol) were added and the reaction was heated under reflux for a further 24 h. Upon cooling, 50 mL of dichloromethane were added and the solution was washed with 2 x 40 mL of deionised water, dried over $MgSO_4$ and concentrated on a rotary evaporator to give a white solid (*O*-benzylparacetamol): 1.20 g, 75.5% yield; mp 140 °C (lit. mp 140 °C.) [18, 27] IR (KBr) 3282 (N-H), 1659 (-NHCO-), 1603, 1527 and 1243 cm^{-1}; ^1H NMR (400MHz, $CDCl_3$) 2.15 (3H, s, -COC**H**$_3$), 5.04 (2H, s, -OC**H**$_2$-), 6.90-6.95 (2H, m, -Ar**H** x 2), 7.04 (1H, br s, -NH-), 7.27-7.34 (1H, m, -Ar**H**), 7.34-7.44 (6H, m, -Ar**H** x 6). *O*-Benzylparacetamol (1.00 g, 4.15 mmol), NaI (0.62 g, 4.15 mmol) and EtBr (0.59 g, 5.39 mmol) were stirred together in 15 mL anhydrous THF with potassium *t*-butoxide (1.40 g, 12.45 mmol). The reaction was carried out at 0 °C under a N_2 atmosphere for 96 h, before quenching *via* the addition of 37% aq. HCl solution. The solution was concentrated to a syrup under reduced pressure and the syrup dissolved in methanol (30 mL). A spatula tip of an amberlyst ion exchange resin (15 hydrogen form) was added in order to neutralise excess potassium *t*-butoxide. Following a 6 h stir, the amberlyst resin was removed by filtration. Deionised water (25 mL) and 25 mL of dichloromethane were added. The aqueous layer was washed a further two times with 25 mL portions of dichloromethane. The organic layers were combined and dried over $MgSO_4$, before concentration under reduced pressure to give a yellow solid which upon analysis was determined to be *N-ethyl-N-(4-hydroxyphenyl)acetamide (28):* 0.22 g, 30% yield; mp 173-175 °C (lit. mp 187-188 °C.) MS (ESI-TOF) m/z: [M + Na]+ Calcd for $C_{10}H_{13}NO_2$; Found 180.1020.. IR (KBr disc) 3200 (O-H stretch), 3109 (Ar C-H stretch), 3024 (Ar C-H stretch), 1668 (amide C=O stretch) and 1514 cm^{-1} (Ar C=C bend). ^1H NMR (400MHz, $CDCl_3$) 1.10 (3H, t, $J_{H\text{-}H}$ = 7.1 Hz, -CH_2C**H**$_3$), 1.82 (3H, s, C**H**$_3$CO-), 3.67-3.74 (2H, m, -C**H**$_2$$CH_3$), 6.86-6.91 (2H, m, -Ar**H** x 2), 6.98-7.03 (2H, m, -Ar**H** x 2).

http://dx.doi.org/10.5772/59715

N-Ethyl-*N*-(4-hydroxyphenyl)acetamide (28) (0.09 g, 0.49 mmol), ethyl iodide (0.075 g, 0.485 mmol) and K_2CO_3 (0.13 g, 0.97 mmol) were stirred in 2 mL of methyl ethyl ketone at r.t. for 14 h, after which one further equivalent of ethyl iodide (0.075 g, 0.485 mmol) was added and the solution was heated at reflux for 2 h. Upon cooling, 5 mL of deionised water was added and the aqueous solution was extracted with 3 x 5 mL portions of diethyl ether. The organic layers were combined, washed with 20 mL of brine and dried over $MgSO_4$, before concentrating under reduced pressure and drying under vacuum for 24 h. *N-Ethylphenacetin (30)* was obtained as thick yellow syrup: 40 mg, 40% yield; HRMS (ESI-TOF) m/z: [M + Na]+ Calcd for $C_{12}H_{17}NO_2Na$ 208.1329; Found 208.1338. ^{1}H NMR (300MHz, $CDCl_3$) 1.02 (3H, t, $J_{H\text{-}H}$ = 7 Hz, -$NCH_2C\mathbf{H}_3$), 1.36 (3H, t, $J_{H\text{-}H}$ = 7 Hz, -$OCH_2C\mathbf{H}_3$), 1.73 (3H, s, $C\mathbf{H}_3CO$-), 3.63 (2H, q $J_{H\text{-}H}$ = 7 Hz, -$OC\mathbf{H}_2CH_3$), 3.97 (2H, q, $J_{H\text{-}H}$ = 7 Hz, -$NC\mathbf{H}_2CH_3$), 6.80-6.86 (2H, m, -Ar**H** x 2), 6.90-7.02 (2H, m, -Ar**H** x 2).

Metastable Zone Width (MSZW) determinations were carried out in a 1L HEL Autolab jacketed glass reaction vessel with Huber P20 silicone thermofluid controlled by a Huber unistat 815 thermoregulator. Agitation was *via* a four blade pitched impeller agitator held at 180 rpm with an overhead motor. Vessel contents temperature was measured by a PTFE PT100 thermocouple. Anti-solvent was added using a ProMinent gamma/L pump. Heating and cooling, agitation and addition of solvent was programmed using HEL WinISO software. Nucleation and particle counts were monitored using a HEL Lasertrack *in situ* laser probe. Ethanol was selected as the crystallising solvent for the MSZW investigation. These involved phenacetin spiked with *N*-ethylparacetamol *(28)* or paracetamol (27) in ratios of 0% (i.e. for determination of the MSZW of pure phenacetin in ethanol) or 1% quantities, and paracetamol in 10% w/w impurity. (It was not feasible to synthesise sufficient quantities of compound (28) for using as an impurity in 10% w/w quantities.) Using the solubility curve for ethanol [13] a saturated solution of phenacetin at 60 °C was prepared. The solution was heated to 70 °C to ensure complete dissolution. The solution was then cooled to 20 °C, at which point 80 g of solvent was added in order to change the concentration. The step was repeated multiple times in order to obtain the MSZW diagrams for spiked phenacetin in ethanol.

Single crystal X-ray goniometer measurements were carried out on a Bruker APEX II DUO diffractometer using the APEX2 v2009.3-0 software [28]. Crystal structure images were prepared using Mercury [29] using the data reported by Hansen et al [19], CSD refcode PYRAZB21.

Serial dissolution study: Growth of large single crystals of phenacetin spiked with paracetamol was accomplished by allowing a spiked solution to concentrate over a period of one week. 50 mg of phenacetin was dissolved in 1.5 mL of ethanol along with 2, 4 and 6 mg of paracetamol in order to obtain 5, 10 and 15% spikes respectively. Gentle heating was required to aid dissolution. Large single crystals were collected and were washed carefully with cold ethanol. Serial dissolution of the spiked phenacetin crystals was accomplished by placing each individual crystal within a glass sample vial and partially dissolving the crystal in methanol-water (40:60). The crystals were firstly weighed (each was typically 4-5 mg) and 1 mL/mg of solvent was used. The crystals were physically removed from the solution upon visual estimation of approximately one third dissolution (typically 1-2 mins.). The crystals were then

transferred to a second and subsequently third vial for further dissolution. The residual solutions were analysed by HPLC as described above.

Co-crystallisation was attempted using physical mixtures of phenacetin and paracetamol in 1:1 and 1:2 ratios. Mixtures recrystallised from ethanol or were ground in a Retsch MM400 ball mill [30].

Acknowledgements

This research has been carried out with the support of the Irish Research Council Enterprise Partnership Scheme (IRSCET-Clarochem-2010-02), Clarochem (Ireland) Ltd., Science Foundation Ireland under Grant Numbers 05/PICA/B802/EC07, 07/SRC/B1158 and 12/RC/2275, and UCC 2013 Strategic Research Fund.

Author details

Danielle E. Horgan, Lorraine M. Crowley, Stephen P. Stokes, Simon E. Lawrence and Humphrey A. Moynihan*

*Address all correspondence to: h.moynihan@ucc.ie

Department of Chemistry / Analytical and Biological Chemistry Research Facility / Synthesis and Solid-State Pharmaceutical Centre, University College Cork, Cork, Ireland

References

[1] U.S. Department of Health and Human Services Food and Drug Administration. ICH Guidance for Industry: Q3A Impurities in New Drug Substances, June 2008. http://www.fda.gov/cder/guidelines.htm

[2] Tanoury GJ, Hett R, Kessler DW, Wald SA, Sennayake CH. Taking Advantage of Polymorphism To Effect an Impurity Removal: Development of a Thermodynamic Crystal Form of (*R,R*)-Formoterol Tartrate. Organic Process Research and Development 2002; 6: 855-862.

[3] Blagden N. Crystal engineering of polymorph appearance: the case of sulphathiazole. Power Technology 2001; 121:46-52.

[4] Solanko, KA, Bond AD. Influence of impurities on the crystallisation of 5-X-aspirin and 5-X-aspirin anhydride polymorphs (X = Cl, Br, Me). CrystEngComm 2011; 13: 6991-6996.

[5] Mukuta T, Lee AY, Kawakami T, Myerson AS. Influence of Impurities on the Solution-Mediated Phase Transformation of an Active Pharmaceutical Ingredient. Crystal Growth and Design 2005; 5: 1429-1436.

[6] Mirmehrabi M, Rohani S, Murthy KSK, Radatus B. Polymorphic Behaviour and Crystal Habit of an Anti-Viral/HIV Drug: Stavudine. Crystal Growth and Design 2006; 6: 141-149.

[7] Berkovitch-Yellin Z, Addadi L, Idelson M, Lahav M, Leiserowitz L. Controlled Modification of Crystal Habit via "Tailor-Made" Impurities. Application to Benzamide. Angewandte Chemie Supplementary 1982; 1336-1345.

[8] Blagden N, Song M, Davey RJ, Seton L, Seaton CC. Ordered Aggregation of Benzamide Crystals Induced Using a "Motif Capper" Additive. Crystal Growth and Design 2005; 5: 467-471.

[9] Fiebig A, Jones MJ, Ulrich J. Predicting the Effect of Impurity Adsorption on Crystal Morphology. Crystal Growth and Design. 2007; 7: 1623-1627.

[10] Moyers CG. Chemical Engineering Progress 1986; 82: 42-46.

[11] Addadi L, Weinstein S, Gati E, Weissbuch I, Lahav M. Resolution of conglomerates with the assistance of tailor-made impurities. Generality and mechanistic aspects of the "rule of reversal". A new method for the assignment of absolute configuration. Journal of the American Chemical Society. 1982; 104:4610-4617.

[12] Weisinger-Lewin Y, Frolow F, McMullan RK, Koetzle TF, Lahav M, Leiserowitz, L. Reduction in crystal symmetry of a solid solution:a neutron diffraction study at 15 K of the host/guest system asparagine/aspartic acid. Journal of the American Chemical Society. 1989; 111:1035-1040.

[13] Moynihan HA, Kelly DM. Phenacetin Crystallization: Cooling Regimes and Crystal Morphology. In: Marcello Rubens Barsi Andreeta (ed.) Crystallization - Science and Technology. Rijeka: InTech; 2012. p329-348.

[14] Clissold SP. Paracetamol and Phenacetin. Drugs 1986; 32(Suppl. 4): 46-59.

[15] Adams R, Johnson RJ, Wilcox CF. Laboratory Experiments in Organic Chemistry, 7th Edition. New York: Macmillan Publishing Co.; 1979.

[16] Eaker CM, Campbell JR. Acetophenetidine. US Patent 2,887,513. May 19, 1959.

[17] Volker EJ, Pride E, Hough C. Drugs in the Chemistry Laboratory. Journal of Chemical Education. 1979; 56(12): 831.

[18] Neubert ME, Norton P, Fishel DL. Molecular Crystals and Liquid Crystals. 1975, 31: 253-257.

[19] Hansen LK, Perlovich GL, Bauer-Brandl A. Redetermination of p-ethoxyacetanilide (phenacetin). Acta Crystallographica E. 2006; E62: o2712-o2713.

[20] Patel U, Patel TC, Singh TP. Structure of phenacetin. Acta Crystallographica C. 1983; C39: 1445-1447.

[21] Etter MC. Encoding and decoding hydrogen-bond patterns of organic compounds. Accounts of Chemical Research. 1990; 23: 120-126.

[22] Haisa M, Kashino S, Kawai R, Maeda H. The Monoclinic Form of *p*-Hydroxyacetamilide. Acta Crystallographica. 1976; B32:1283-1285.

[23] His KH, Kenny M, Simi A, Myerson AS. Purification of Structurally Similar Compounds by the Formation of Impurity C-Former Complexes in Solution. Crystal Growth and Design. 2013; 13: 1577-1582.

[24] Weber CC, Wood GPF. Kunov-Kruse AJ, Nmagu DE, Trout BL, Myerson AS. Quantitative Solution Measurement for the Selection of Complexing Agents to Enable Purification by Impurity Complexation, Crystal Growth and Design. 2014; 14: 3649-3657.

[25] Oswald IDH, Allan DR, McGregor PA, Motherwell WDS, Parsons S, Pulham CR. The formation of paracetamol (acetaminophen) adducts with hydrogen-bond acceptors. Acta Crystallographica Section B 2002; 58: 1057-1066.

[26] Maeno Y, Fukami T, Kawahata M, Yamaguchi K, Tagami T, Ozeki T, Suzuki T, Tomono K. Novel pharmaceutical cocrystals consisting of paracetamol and trimethylglycine, a new promising cocrystals former. International Journal of Pharmaceutics 2014; 473: 179-186.

[27] Rastogi N, Kant P, Sethi R, Shukla S, Harrison DA. Synthesis of a series of aminomethylated 5-nitro-1H-benzo[d]imidazoles, 6-nitrobenzo[d]oxazol-2(3H)-ones and 4-nitroisoindoline-1,3-diones as antileishmanial and antimicrobial agents. Indian Journal of Heterocyclic Chemistry 2010; 2092): 149-152.

[28] APEX2 v2009.3-0. Bruker AXS: Madison, WI, 2009.

[29] Macrae CF, Bruno IJ, Chisholm JA, Edginton PR, McCabe P, Pidcock E, Rodriguez-Monge L, Taylor R, van de Streek J, Wood PA, Journal of Applied Crystallography. 2008, 41: 466-470.

[30] Eccles KS, Morrison RE, Stokes SP, O'Mahony GE, Hayes JA, Kelly DM, O'Boyle NM, Fabian L, Moynihan HA, Maguire AR, Lawrence SE. Utilizing Sulfoxide...Iodine Halogen Bonding for Cocrystallization. Crystal Growth and Design. 2012; 12: 2969-2977.